Bioresource Technology, Volume 266, Issue October, 2018, Pages 463-471
DOI:10.1016/j.biortech.2018.06.096

Influence of carrier media physical properties on start-up of moving attached growth systems

Joana Dias[a], Mell Bellingham[b], Junaid Hassan[b], Mark Barrett[b], Tom Stephenson[a], Ana Soares[a]

[a] *Cranfield University Water Sciences Institute, Cranfield, MK43 0AL, UK.*

[b] *Warden Biomedia, 31 Sundon Industrial Estate, Dencora Way, Luton, Bedford, LU3 3HP, UK.*

Graphical abstract:

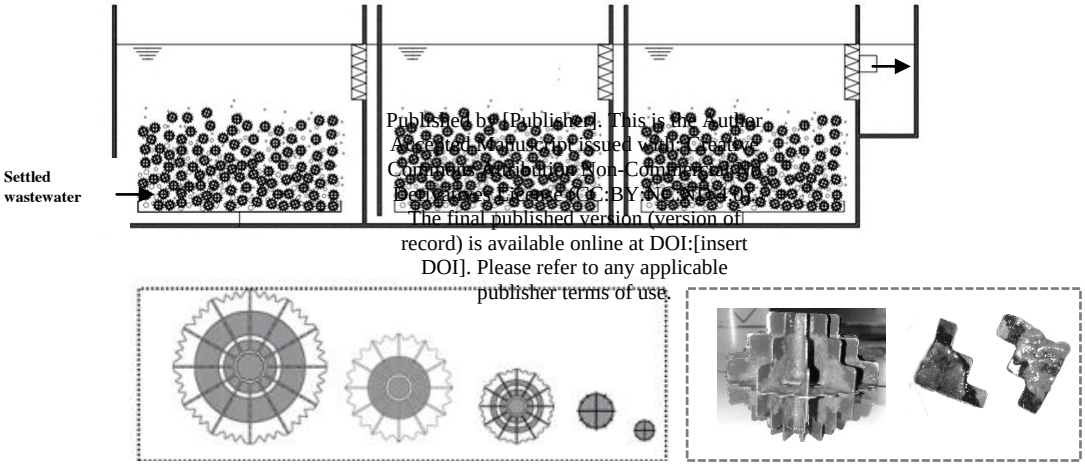

Influence of carrier media physical properties on start-up of moving bed biofilm systems

Joana Dias[a], Mell Bellingham[b], Junaid Hassan[b], Mark Barrett[b], Tom Stephenson[a], Ana Soares[a*]

[a] *Cranfield University Water Sciences Institute, Cranfield, MK43 0AL, UK.*

[b] *Warden Biomedia, 31 Sundon Industrial Estate, Dencora Way, Luton, Bedford LU3 3HP, UK*

Highlights:

- Three spherical and two cylindrical shaped carrier media were tested.
- Faster biofilm formation rates were observed with the spherical carrier media.
- Larger voidage of the spherical carrier media improved COD and ammonia removal.
- Carrier media physical properties and hydraulic efficiency played a role on start-up.
- Start-up was not a function of carrier media protected surface area.

Influence of carrier media physical properties on start-up of moving attached growth systems

Joana Dias[a], Mell Bellingham[b], Junaid Hassan[b], Mark Barrett[b], Tom Stephenson[a], Ana Soares[a*]

[a] *Cranfield University Water Sciences Institute, Cranfield, MK43 0AL, UK.*

[b] *Warden Biomedia, 31 Sundon Industrial Estate, Dencora Way, Luton, Bedford, LU3 3HP, UK.*

Abstract

Five carrier media with different shapes (spherical and cylindrical), sizes, voidage and protected surface areas (112-610 m^2/m^3) were studied in a pilot scale moving bed biofilm reactor (MBBR). This study aimed at assessing start-up duration using biofilm formation rates. Results indicated that the spherical media required shorter periods to achieve stable biofilm formation rates associated with chemical oxygen demand (COD) (15-17 days), compared to cylindrical high surface area media (23-24 days). Protected surface area presented weaker correlations with the biofilm formation rate for COD (R^2= 0.83) and ammonia removal (R^2= 0.76). However, good correlations were observed with a combination of the media physical factors: dimensionality (Di), voidage (Voi), and hydraulic efficiency (HE) strongly correlated with biofilm formation rates for heterotrophic (R^2= 0.95) and nitrifying bacteria (R^2= 0.92). This study proposes that the media physical properties can contribute to shortening start-up, contributing to improved removal rates and fast commissioning of MBBRs.

Keywords: Biofilm formation rate, biofilm detachment, dimensionality, moving attached growth, start-up, voidage.

*Corresponding author at Cranfield Water Science Institute, Cranfield University, Vincent Building, Cranfield, Bedfordshire, MK43 0AL, UK. Tel.: +44 (0) 1234 758121. E-mail address: a.soares@cranfield.ac.uk (A. Soares).

1. Introduction

The need to meet increasingly stringent discharge limits has made biofilm processes popular for the removal of organic pollutants and nitrogen in wastewater treatment plants (WWTPs) (Barwal and Chaudhary, 2016). Moving bed biofilm systems, such as submerged aerated filters (SAFs) (structured or random packed) (Holloway and Soares, 2018), moving bed biofilm reactor (MBBRs) and integrated fixed film activated sludge (IFAS) use buoyant carrier media as a biofilm growth support material. MBBRs have been established in the past 25 years as robust, versatile and compact solutions and have been successfully implemented in municipal and industrial wastewater treatment (Leyva-Díaz et al., 2013; Ødegaard, 2016).

The initial biofilm adhesion plays a crucial role on attached growth systems (Mao et al., 2017; Tang et al., 2017). Due to the nature of the process the time required to achieve a well-established biofilm can vary considerably from 1 to 6 weeks (Bassin et al., 2016; Dong et al., 2015; Leyva-Díaz et al., 2013; Tang et al., 2016). Start-up duration has been a major drawback on full-scale applications especially in nitrification processes (Lackner et al., 2009) due to the slow growth rate of nitrifiers (Habouzit et al., 2014; Rikmann et al., 2018; Zekker et al., 2016).

Bacterial adhesion to support surfaces has been extensively studied, and physical (size, shape, density, roughness) and chemical properties (surface materials: plastic, foam, woven, ceramic, glass, etc. and chemical modified polymer) have been shown to strongly affect early stages of biofilm formation (Deng et al., 2016; Eldyasti et al., 2012). Biofilm formation occurs after initial cell adhesion to the surface of the carrier media that then leads to bacteria accumulation and extracellular polymeric substances (EPS) production. This helps bacteria

bind and form the biofilm (Zhu et al., 2015). However, bacterial adhesion and subsequent biofilm development is a dynamic process that can be affected by external factors such as operating conditions, organic and nutrient loading and hydrodynamics within the reactor (Liu and Tay, 2002; Pellicer-Nàcher and Smets, 2014). The latter plays a critical role during start-up as it controls biofilm detachment caused by shear forces (superficial air velocity) and abrasion (carrier media concentration) (Goel et al., 2011; Mao et al., 2017). To ensure a fast-start up and stable biofilm formation a balance has to be achieved between biofilm growth and detachment processes (Lackner et al., 2009).

To date, there have been limited studies on start-up of moving attached growth systems (Zekker et al., 2012). Most studies identified in the literature are performed at the laboratory scale, and focus on strategies to accelerate the adhesion of the microorganisms, to the carrier reducing the start-up duration. Zhu et al. (2015) fed a 9 L laboratory scale reactor with easy biodegradable substrates (synthetic wastewater) inoculated with activated sludge from a secondary clarifier. The reactor was used to describe different start-up stages in biofilm systems with a cylindrical shape carrier media with a protected surface area of 460 m^2/m^3 (no information provided about the carrier media material). Stable COD and ammonia removals of 92% and 50% were achieved after 6 and 14 days of start-up respectively (Zhu et al., 2015). The same strategy was used by Bassin et al. (2016) on the start-up using two different carrier media; a cylindrical (high density polyethylene) and chip shaped (virgin polyethylene with additives) media with 500 and 3000 m^2/m^3 at 50 and 8.3% filling ratio. Twenty to thirty days were necessary for a constant attached biofilm to be achieved. Seeding sludge and synthetic wastewater was also used in Mao et al. (2017) where start-up was compared using three high

density polyethylene (HDPE) carriers (two modified and one unmodified). Modified material using PQAS-10 polyquaternium-10 and cationic polyacrylamides (CPAM) resulting in 13, 19 and 27 days, respectively. Batch feeding and prolonged hydraulic retention times were adopted as a start-up strategy in Tang et al. (2016) using a round polyethylene ball and start-up was achieved in only 6 days. These studies mainly demonstrate the dynamic nature of the process but also highlight the variation of how start-up is interpreted and defined. Start-up in moving attached growth systems has been described in a multitude of parameters, including: biofilm growth, time to form a fully developed biofilm, biofilm activity and reactor performance (i.e. substrate removal efficiencies) (Bassin et al., 2016; Mao et al., 2017; Tenno et al., 2016; Zekker et al., 2017; Zhu et al., 2015)

Research on moving attached growth system start-up has been limited so far and to date, no studies have investigated the relationships between carrier media physical properties and start-up. The significance of this is emphasised in the importance of start-up towards achieving low commission periods and treatment robustness during steady state (Rikmann et al., 2014; Zekker et al., 2012).

This in turn can lead to improvement of the economic competitiveness of the moving attached growth system technology. Therefore, this study aims to investigate how carrier media physical properties influence process start-up using real wastewater. The expected outcome of this work is intended to provide guidance for design and start-up of a full-scale moving attached growth system plant. Furthermore, the fast biofilm formation rate, can be of benefit for operation conditions modification (increased flow and organic loading) as well as

for upgrade of existing wastewater treatment plants contributing to the extended application of moving attached growth systems.

2. Material and methods

2.1. Pilot plant setup and operation conditions

A 2 m^3 rectangular shaped pilot plant divided into three separate aerobic cells of equal volume (1.0 m width x 1.5 m length and 1.30 m height), was designed to study process start-up. Medium bubble aeration was utilised to supply the required aeration and mixing. The pilot was designed to cope with variable air velocities 3.6-18.7 m^3/m^2.h and wastewater flows, ranging from 2.5-18 m^3/day. Air and wastewater flows were normalised per protected surface area of media. Wastewater distribution was enhanced by the instalment of two baffles on the cells. The five carrier media with different physical properties investigated were supplied by Warden Biomedia (Table 1). Media 1, 2 and 3 were spherical media with a protected surface area of 112, 149 and 220 m^2/m^3 respectively whilst Media 4 and 5 were cylindrical in shape with a protected surface area of 350 and 610 m^2/m^3 (Table 1). The pilot plant was fed with settled wastewater from Cranfield University wastewater treatment plant (Cranfield, UK) during 2016-2018. Each media was study for 60 days, covering a total of 300 days for the 5 media. The organic and nutrient loading per surface area was kept constant by fixing the media filling ratio at 60%, within the values recommended in literature (McQuarrie and Boltz, 2011), by varying the wastewater flow rate. The pilot-plant was designed to keep stable dissolved oxygen levels by delivering variable air flow velocities (between 3.6-18.7 m3/m2.h) and variable wastewater flow (between 2.5-18.0 m3/day). The start-up was done with clean media directly transferred to the tank. No foam formation was observed.

2.2. Chemical analysis

The wastewater of the influent and effluent was sampled three times a week during process start-up.

Samples were analysed for total 5-day carbonaceous biochemical oxygen demand (BOD_5) and soluble BOD_5, total and volatile suspended solids (TSS and VSS) according to standard methods (APHA, 2005). Total and soluble chemical oxygen demand (tCOD and sCOD), ammonium-nitrogen (NH_4^+-N), and nitrate-nitrogen (NO_3^--N) were analysed using Merck cell tests kits (Merck KGaA, Darmstadt, Germany) and measured with a NOVA60 photometer (VWR, UK). Temperature, dissolved oxygen (DO) and pH were measured onsite daily using portable meters (HACH HQ40d; Camlab, Cambridge, UK).

Statistical analysis was completed using the software IBM SPSS Statistics 23 and results checked for normality using Shapiro-Wilk tests. ANOVA tests were applied for the normal distributed data. Statistical differences were based on 95 % of the confidence level ($p<0.05$).

Attached growth biofilm on the carriers was analysed two to three times a week following the procedure described in Regmi et al. (2011). Carriers were sampled and dried at 105ºC overnight and weighed. The biofilm was removed by placing the carriers in a H_2SO_4 solution (2 N) and stirred vigorously for 24 hours. The carriers were washed with tap water then biofilm brushed off and dried at 105ºC. The total attached biofilm was calculated based on the difference in media dry weight before and after removing all biofilm attached. The results were expressed as grams of total solids per metre square of protected surface area of carrier media (g TS/m^2). Carriers were sampled from the three cells of the pilot plant (10 carriers of Media 1, 2 and 3 and 40 carriers of Media 4 and 5).

Protected surface area was defined in this study as the area of carrier covered with biofilm. The protected surface area was calculated for each media. Individual carriers were cut and separated into small pieces and photographed. Comparisons were made between the area covered with biofilm and the area without biofilm attached. All the images were analysed using ImageJ Software and biofilm coverage area determined.

Organic removal performance was evaluated according to Ødegaard (Ødegaard, 2006). An "obtainable removal rate" was calculated based on 100% solids separation. Influent tCOD and effluent sCOD were compared with flow and protected surface area.

Equation (1) was used to fit a curve to the attached biofilm measured (Szilágyi et al., 2013). Where *m(t)* is the attached biofilm as a function of time, m_{max} the maximum amount of biofilm and K_m coefficient of growth. The curve was fitted by manipulating the K_m in order to obtain the best fitted curve (Szilágyi et al., 2013).

$$m(t) = m_{max}\frac{t}{K_m + t} \quad \textbf{(1)}$$

Biofilm thickness was measured through Optical Coherence Tomography (OCT) using a Thorlabs Standard (SR-OCT 930nm; Thorlabs. Germany), with a refractive index of 1.33 (water). The media was cut into small pieces with a surgical scalpel and 20 images captured from different pieces of the carriers. Biofilm thickness was estimated based on the average of 60 measurements.

Extracellular polymeric substances (EPSs) were determined following biofilm detachment from the media using the methodology described by Le-Clech et al. (2006). Carbohydrate and protein concentrations were determined according to the Dubois phenol-

sulphuric acid method (UV490 nm) with D-glucose (Acros Organics, UK) as the standard (Dubois et al., 1956) and Protein by the Folin method (UV750 nm) with bovine serum albumin (BSA) (Sigma-Aldrich, UK) as the standard (Lowery et al., 1951) respectively.

Observed yields were calculated based on Eldyasti et al. (2012) using the linear regression between the cumulative production of volatile suspended solids (VSS) in the effluent and the cumulative COD removed ($tCOD_{in}$-$sCOD_{out}$).

The detachment coefficient (k_{de}) was estimated using the equation described in Patel et al. (2005) and Eldyasti et al.(2012) (Equation 2).

$$k_{de} = \frac{Q \times [VSS_{out}]}{A \times M_t} \quad \textbf{(2)}$$

Where, VSS_{out} is the solids leaving the pilot plant and Q is the flow rate, M_t is the biofilm attached per protected area of carrier media and A is the media protected surface area.

3. Results and discussion

3.1. Performance of moving attached growth system during start-up

The temperature within the cells varied from 18.6±1.9, 19.8±2.3, 20.2±0.6, 17.1±1.3 and 14.6±1.2˚C during operation with Media 1, 2, 3, 4 and 5, respectively (Table 2) due to natural annual wastewater temperature fluctuations. Temperature for Media 5 was statistically different from Media 1, 2, 3 and 4 ($p \leq 0.05$). The average total COD influent varied 389±71, 257±44, 305±32, 236±15 and 251±24 mg/L for Media 1 to 5, respectively. Ammonia concentration varied from 35±5, 34±11, 36±3, 38±6 and 31±5 mg NH_4^+-N/L for Media 1 to 5, respectively. Natural wastewater variability resulted in changes in the COD and ammonia concentrations fed to the pilot plant. The average surface organic loading rate varied between

8.7±1.6, 6.8±1.2, 8.3±0.9, 6.8±0.4 and 7.0±0.7 g total COD/m^2.day for Media 1, 2, 3, 4 and 5, respectively (Table 2). Nevertheless, the organic loading rates were statistically similar during the operation with the various media (except for Media 1, which had a different COD loading rate, $p \leq 0.05$, compared with the other media, but the total BOD_5 was statistically similar). Ammonia loadings varied from 0.8±0.1, 0.9±0.3, 1.0±0.1, 1.1±0.1 and 0.9±0.1 g NH_4^+-N/m^2.day for Media 1, 2, 3, 4 and 5 respectively. There was no statistical difference between the five media for ammonia loading. The DO was maintained at 4.1±1.03, 4.0±1.2, 3.0±0.6, 5.1±1.6 and 3.2±1.1 mg O_2/L in Cell 1 and 5.6±0.5, 6.1±0.9, 6.9±1.2, 5.6±1.1 and 6.6±1.0 mg O_2/L in Cell 3.

The COD removal efficiency and biofilm formation was tracked during the first 60 days of operation. After 6 days of operation the COD removal was high with values of 78, 82, 78, 75 and 79% with Media 1, 2, 3, 4 and 5, respectively (Fig. 1). The COD removal efficiencies reached stable values of 88±4% in Media 1 (after day 18), 81±4% in Media 2 (after day 15), 85±3% in Media 3 (after day 17), 80±3% in Media 4 (after 23 days) and 86±4% in Media 5 (after 24 days) (Fig. 1a).

Throughout the first 10 days of operation, ammonia removal efficiencies were low for all media, with values reaching 24±7, 33±17, 31±15, 24±11 and 19±11% for Media 1 to 5, respectively. Media 1, 2 and 3 (spherical shape) achieved ammonia removal efficiencies of 50±13, 64±13, 63±7% after 30, 22 and 17 days, respectively. Media 4 and 5 (cylindrical shape) achieved ammonia removal efficiencies of 32±17% after 46 days and 34±5% after 47 days, respectively (Fig. 1b).

Ammonia removal rates were 0.4±0.1 g NH_4^+-N/m^2.day (30 days), 0.5±0.1 g NH_4^+-N/m^2.day (22 days), 0.7±0.1 g NH_4^+-N/m^2.day (17 days), 0.2±0.1 g NH_4^+-N/m^2.day (46 days) and 0.3±0.1 g NH_4^+-N/m^2.day (47 days) for Media 1, 2, 3, 4 and 5, respectively. It is likely that low nitrification was impacted by the concentration of organic matter (BOD) reaching the third cell. Organic loadings were also measured in the different cells during operation. The third cell organic loading rates was 1.4±0.9, 1.6±0.9, 2.1±1.0, 2.8±0.9 and 2.9±0.7 g BOD_5/m^2.day when the reactor was operated with Media 1, 2, 3, 4 and 5 respectively. Higher loadings verified in Cell 3 when Media 4 and 5 were used, 2.8±0.9 and 2.9±0.7 g BOD_5/m^2.day, respectively. Suggesting that with Media 4 and 5, a lower organic removal occurred in Cell 1 and 2, as the loading rates were kept constant at the influent. The organic loading rate for Cell 3 for Media 4 and 5 were slightly higher than those recommended by Hem et al. (1994) of approximately < 2 g BOD_5/m^2.day. The presence of organics, in the third cell, had promoted growth of heterotrophs and competing nitrifiers slowing down nitrification (Hem et al., 1994). A similar finding was reported by Zhu et al. (2015), which registered only 50% ammonia removal after 14 days of operation, and the low nitrification was attributed to the high carbon: nitrogen ratio (C/N). From the data reported in the literature, the range of temperatures measured did not indicate nitrification to be impacted by temperature (temperatures in Cell 3 for Media 4 and 5, 17.1±1.3 and 14.6±1.2˚C respectively) (Salvetti et al., 2006). This is supported by other researchers who have indicated no significant impact on nitrification rate at temperatures of 14, 20 and 27˚C with maximum ammonia removal of 1.69, 1.72 and 1.86 g/m^2.day, respectively (Zhu and Chen, 2002; Daija et al., 2016).

3.2. Biofilm formation and start-up

In this study, process start-up was defined as the period of time for biofilm formation rates to reach stable values. Bacterial adhesion was observed after the second day of operation, and values of 0.67, 0.90, 1.21, 1.44 and 1.40 g TS/m^2 were measured in Media 1, 2, 3, 4 and 5, respectively (Fig. 2a). This can be defined as the 1st stage of biofilm formation (Zhu et al., 2015).The biofilm continued developing gradually until day 18, 15, 17, 23 and 24 for Media 1, 2, 3, 4 and 5, respectively, when the attached biofilm reached stable values (8.73, 8.66, 8.79, 8.09 and 6.38 g TS/m^2 for Media 1, 2, 3, 4 and 5, respectively) (Fig. 2a). This corresponds to the 2nd and 3rd stages of biofilm growth and accumulation respectively. The biofilm formation rate was calculated based on the slope of the biofilm attachment until it reached stable values (Fig. 2b). The estimated biofilm formation rates during start up were 0.50, 0.52, 0.55, 0.36 and 0.27 g TS/m^2.day for Media 1, 2, 3, 4 and 5, respectively. The results clearly indicate that the biofilm formation rate was faster on spherical media, with higher voidage and diameter, compared with the cylindrical media, with lower voidage and higher surface area. Di Trapani et al. (2008), stated that one month was required to reach stable conditions, with an attached biofilm of around 11.57 g TS/m^2 and 15.15 g TS/m^2 at 35 and 65% filling ratio, respectively using a cylindrical shape carrier media. Falletti et al. (2014) observed a visibly fully grown biofilm after five weeks of operation (39.3 g TSS/m^2) using a cylindrical media. Dong et al. (2015), considered that biofilm was stable and mature in 25 days with a hollow spherical honeycomb and a cylindrical shape carrier media, with attached biofilm of 0.04 g/cm^3. With pre-settled wastewater, Siciliano and De Rosa (2016) observed that heterotrophic biofilm start up required seven days reaching a 3 g TS/m^2 of

attached biofilm in a cylindrical shape carrier media. Bassin et al. (2016) observed, after 20 and 30 days of start-up, a biofilm attached concentration of 13 g TS/m^2 in a 500 m^2/m^3 cylindrical shape carrier media and 7 g TS/m^2 in a 3000 m^2/m^3 chip shaped carrier media.

For the nitrification process start-up in Cell 3, bacteria attachment was observed on the second day of operation with 0.54, 0.31, 0.45, 0.33, 0.48 g TS/m^2 for Media 1 to 5, respectively. The biofilm continued to increase until it attained stabilisation around day 30, 22, 17, 46 and 47 for Media 1, 2, 3, 4 and 5, respectively (6.56, 5.48, 3.83, 9.34, 7.57 g TS/m^2, Media 1 to 5, respectively) (Fig. 3a). Others have reported average values of 7 g TSS/m^2 after 1 month on a nitrifying integrated fixed-film activated sludge system (IFAS) start-up using cylindrical shaped carrier media (Regmi et al., 2011). In Bassin et al. (2012) two months were required to start-up a reactor operating under autotrophic conditions using a cylindrical shaped carrier media.

The biofilm formation rate was determined based on the slope of the biofilm attached until stable values were reached, from day 0 to day 30, 22,17, 46 and 47. These estimated values were 0.21, 0.24, 0.22, 0.18, 0.17 g TS/m^2.day for Media 1, 2, 3, 4 and 5 respectively (Fig. 3b). The biofilm formation rate is usually linked with the nitrification rate (Wiesmann, 1994). Spherical shape media achieved higher ammonia removal efficiencies (Fig. 3b) and thus a higher biofilm formation rate than cylindrical media.

The biofilm thicknesses in Cell 1 were 36, 51, 84, 50 and 82 μm on the second day, for Media 1 to 5, respectively (Fig. 4a). The biofilm thickness reached stable values at 225±52, 172±25, 195±35, 250±73 and 190±63 μm for Media 1, 2, 3, 4 and 5 at day 18, 15, 17, 23 and 24, respectively (Fig. 4a). For the cylindrical media, the biofilm was mainly situated in the

internal fins, in the small ridges of the media and the biofilm thickness attained values between 365-465 μm and 224-361 μm for Media 4 and 5, respectively, by the end of start-up. The biofilm in Media 1, 2 and 3 was spread uniformly. In Cell 3, aimed at ammonia removal, the initial biofilm thickness was 22±24, 31±30, 39±14, 19±10 and 28±11 μm for Media 1, 2, 3, 4 and 5, respectively. The thickness increased to values of 130±25, 71±22, 86±29, 190±50 and 149±47 μm at day 30,22,17, 46 and 47, respectively (Fig. 4b).

Protected surface area of each media was estimated at the macroscopic scale with photography. In Media 1 (large spherical shape), the biofilm was distributed evenly over the media. Approximately 83% of the carrier media area was covered with biofilm, giving a protected surface area of 112 m^2/m^3. For Media 2 and 3 (medium and smaller spherical media) the biofilm was mainly situated in the internal fins, covering 68 and 71% of the total area (protected surface area of 148 and 220 m^2/m^3, respectively). In Media 4 and 5 (cylindrical shape) the biofilm was located exclusively on the internal fins. No biofilm attachment was verified on the external surface of Media 4 and 5. As such 58 and 61% of Media 4 and 5 were covered with biofilm, yielding a protected surface area of 348 and 610 m^2/m^3, respectively.

During the first days of operation, a similar EPS profile was observed for all the media in Cell 1 (organic removal). The EPS concentration increased, reaching values of 20.6±0.4, 21.3±0.3, 28.3±0.1, 28.2±0.75 and 27.4±0.81 mg tEPS /g VSS for Media 1, 2, 3, 4 and 5, respectively (Fig. 5a). As expected, the EPS production was higher throughout the first days of operation due to the adhesion phenomena and interaction between the heterotrophic bacteria and the carrier surface (Badireddy et al., 2010). A gradual increase in total EPS was

also observed in Tang et al. (2017) with values of 15, 22, 32.5 and 38 mg tEPS /g VSS measured at the initial stage of biofilm formation (0, 3, 11, 18 and day 25 days). Similar observations, also identified by Tang et al. (2015) demonstrated an increase from 30 mg EPS /g VSS on day 5 up to 250 mg EPS/g VSS on day 27. In Oberoi and Philip (2017) the concentration of EPS increased from 36.8 to 72.2 mg EPS/g VSS at the end of start-up. Total EPS content in an IFAS varied from 44 to 71 mg tEPS/g VSS using different media (Mahendran et al., 2012).

A gradual decrease in EPS concentration was observed after the first week and values stabilised at 16.0±0.4, 18.2±0.9, 9.18±0.1, 11.83±0.9 and 12.83±0.2 mg tEPS/g VSS on day 16, 15, 19, 17 and 16 for Media 1, 2, 3, 4 and 5, respectively. As predicted the values of EPS decreased after bacteria adhesion and growth. As the biofilm grows in thickness, diffusion becomes critical, and cells start to grow slower reducing EPS production and biofilm cohesion resulting in biofilm detachment (Ahimou et al., 2007). After day 25 a gradual decrease in EPS production was also observed in Tang et al. (2017) during the maturity and detachment phases.

The total EPS associated with the biofilm in Cell 3 of the pilot plant during the first days of operation were 22.1±0.5, 22.5±0.4, 20.1±0.3, 27.3±0.6 and 34.8±1.9 mg tEPS/g VSS for Media 1, 2, 3, 4 and 5, respectively (Fig. 5b). Similarly, the EPS decreased as operation progressed. After days 30, 22, 17, 46 and 47 days of operation, the EPS were 17.2±0.3, 5.7±0.3, 6.6±0.1, 10.6±0.1 and 9.7±0.3 mg tEPS/g VSS for Media 1, 2, 3, 4 and 5, respectively. Values of EPS were very similar between the first cell and third cell. Nonetheless, nitrifiers are slow growing bacteria with low EPS production compared to

heterotrophic bacteria. The high EPS formation in Cell 3, might have been produced by heterotrophic bacteria due to the high COD reaching the third cell during start-up. Bassin et al. (2012) stated that EPS produced by heterotrophic bacteria were utilised by nitrifiers for biofilm formation during start-up.

During start up the biofilm attached on carrier per amount of COD converted was compared between media. Values of 0.26, 0.27, 0.28, 0.65 and 0.41 g VSS/g COD were calculated in Media 1, 2, 3, 4 and 5, respectively (Fig. 6a). The higher biomass yield achieved in media 4 and 5 correlated well with the lower biofilm formation rate estimated during the start-up period. Values of 0.5 g SS/g filtered COD are reported on the literature (Ødegaard, 2006). An initial detachment rate coefficient was calculated based on a mass balance between the solids leaving the reactor and the biofilm attached per area of carrier media (Eldyasti et al., 2012). The normalised average detachment rate (1/d) was compared between media, and the attached biofilm considered for COD removal was from Cell 1 of the reactor. Due to the dynamic of biofilm accumulation in moving attached growth systems, detachment rates displayed significant variations during the start-up for all the five media studied. Values of 0.24±0.10, 0.29±0.14, 0.37±0.18, 0.80±0.25 and 0.66±0.25 1/d were measured in Cell 1 for Media 1 to 5, respectively (Fig. 6b). Media 4 and 5 (cylindrical shape) promoted higher detachment due to interaction with aeration during initial biofilm formation, while the open spherical structure of Media 1, 2 and 3 enhanced initial biofilm formation, protecting the biofilm from shear. Values of 0.12 g VSS/g COD and detachment rates of 0.05 1/d were reported in Eldyasti et al. (2012) for a high spherical media compared with 0.19 g VSS/g COD and detachment rates of 0.17 1/d for a low sphericity media.

4. Influence of the media physical properties on start-up duration

In moving attached growth systems, the main factor assuring a fast start-up is the biofilm development. In this study start-up duration was assessed based on the attached biofilm (g TS/m^2). In order to study the influence of media physical properties on the pilot plant start-up, the biofilm formation rate was correlated with media physical properties. The media physical properties were previously identified in Dias et al. (2018), to correlate with process hydrodynamics and oxygen mass transfer. More specifically, media dimensionality (Di) and voidage (Voi) were found to strongly correlate with oxygen mass transfer (R^2= 0.89) and pilot plant hydraulic efficiency (HE) (R^2= 0.92) both in clean media and with biofilm attached to the media (Dias et al., 2018). Hydraulic efficiency (HE) was determined through tracer studies using Rhodamine and calculated based on the ratio between mean residence time and hydraulic retention time (tm/HRT).

When the rate of biofilm formation in Cell 1 (COD removal) and Cell 3 (ammonia removal) was compared with the media protected surface area, good correlations were achieved (R^2 of 0.83 and R^2 of 0.76, respectively) (Fig. 7a). A stronger correlation was identified between the combination of parameters (Di x Voi)/HE, and the rate of biofilm formation during COD removal start up (R^2= 0.95) and an R^2 of 0.92 during ammonia removal start-up (Fig. 7b).

The physical media properties and hydraulic efficiency clearly demonstrate the importance of media shape and size on biofilm attachment and start-up. Biofilm formation rates were 30±1% higher in the spherical media during organic removal start-up and 20±3% higher during ammonia removal start-up, when compared with cylindrical media. The high voidage (95, 92 and 90%) and open structure of spherical media (Media 1, 2 and 3) was

associated with higher hydraulic efficiencies (89±2, 93±5 and 100%) as outlined in Dias et al. (2018). This led to increased oxygen mass transfer offering better conditions for biofilm to attach, leading to a faster start-up. In turn this provided, improved mass transfer at the bulk/biofilm interface increasing biofilm activity and treatment performance (Tang et al., 2017). The reduction on hydraulic efficiencies and media voidage, obtained with cylindrical media (Media 4: HE 74±1% and Voi reduction of 6%; Media 5: HE 63±2% and Voi reduction of 14%) (Dias et al., 2018), explained the longer start-up (46 and 47 days).

The diffusion of oxygen is usually limited after a critical biofilm thickness of 50-150 μm (Syron and Casey, 2008). Values of biofilm thickness of 190±50 and 149±47 μm were measured in Media 4 and 5 during start-up. Despite the higher protected surface area of Media 4 and 5 the start-up duration and biofilm formation rate were slower compared with the lower protected surface area (Media 1, 2 and 3). This confirms the contribution and the important roles played by other properties in the media. Similar observations were stated in Bassin et al. (2016) where higher attached biofilm concentrations were reached in a smaller protected surface area media compared with higher protected surface area media. In Eldyasti et al. (2012) work, surface shape (sphericity), played an important role on biofilm structure with 70% lower biofilm yield and detachments rate observed on high sphericity media (0.9) compared to low sphericity media (0.5).

The open spherical structure of Media 1, 2 and 3 notwithstanding the lower protected surface area, favoured wastewater circulation and oxygen distribution within all areas of the media. Therefore, this study highlights the importance of media physical properties on biofilm growth and retention and their impact on the start-up duration on moving attached

growth systems. The knowledge gained through this study will challenge current literature knowledge and commercial strategies that appointed the protected surface area as the key factor for the design and operation of moving attached growth system (Ødegaard et al., 2000). Findings highlighted the importance of voidage on biofilm growth and maintenance and thus on treatment performance during start-up.

Hence, considering the importance of start-up to achieve stable operational performance at low commission periods, the economic competitiveness of the moving attached growth system technology can be improved through additional focus on carrier media properties (voidage and shape).

5. Conclusions

In this study, the influence of carrier media physical properties on the start-up duration of a moving attached growth system was investigated. Start-up was monitored using the biofilm formation rate. Faster biofilm formation rates were obtained for COD removal and ammonia removal when spherical media was used. Stronger correlations were observed between the biofilm formation rates and the combination of physical factors and hydraulic efficiency (Di x Voi)/HE for COD and ammonia removal rates. This study highlighted that the conventional way to design moving attached growth systems should not be exclusively according to its protected surface area and future moving attached growth system design and evaluation should focus equally on carrier media physical properties.

Acknowledgements

The authors acknowledge the financial support from Warden Biomedia and Cranfield University.

Appendix A. Supplementary data

Supplementary data associated with this article can be found

References

Ahimou, F., Semmens, M.J., Haugstad, G., Novak, P.J., 2007. Effect of protein, polysaccharide, and oxygen concentration profiles on biofilm cohesiveness. Appl. Environ. Microbiol. 73, 2905–2910.

APHA, 2005. Standard Methods for the Examination of Water and Wastewater, 21st ed. American Public Health Association, Washington, D.C.

Badireddy, A.R., Chellam, S., Gassman, P.L., Engelhard, M.H., Lea, A.S., Rosso, K.M., 2010. Role of extracellular polymeric substances in bioflocculation of activated sludge microorganisms under glucose-controlled conditions. Water Res. 44, 4505–4516.

Barwal, A., Chaudhary, R., 2016. Feasibility study for the treatment of municipal wastewater by using a hybrid bio-solar process. J. Environ. Manage. 177, 271–277.

Bassin, J.P., Dias, I.N., Cao, S.M.S., Senra, E., Laranjeira, Y., Dezotti, M., 2016. Effect of increasing organic loading rates on the performance of moving-bed biofilm reactors filled with different support media: Assessing the activity of suspended and attached biomass fractions. Process Saf. Environ. Prot. 100, 131–141.

Bassin, J.P., Kleerebezem, R., Rosado, A.S., Van Loosdrecht, M.C.M., Dezotti, M., 2012. Effect of different operational conditions on biofilm development, nitrification, and nitrifying microbial population in moving-bed biofilm reactors. Environ. Sci. Technol. 46, 1546–1555.

Daija, L.; Selberg A., Rikmann E., Zekker I., Tenno T., Tenno T., 2016. The influence of lower temperature, influent fluctuations and long retention time on the performance of an upflow mode laboratory-scale septic tank. Desal and Water Treatme. 57,1-9.

Deng, L., Guo, W., Ngo, H.H., Zhang, X., Wang, X.C., Zhang, Q., Chen, R., 2016. New functional biocarriers for enhancing the performance of a hybrid moving bed biofilm reactor-membrane bioreactor system. Bioresour. Technol. 208, 87–93.

Dias, J., Stephenson, T., Bellingham, M., Hassan, J., Barrett, M., Soares, A., 2018. Impact of carrier media on oxygen transfer and wastewater hydrodynamics on a moving attached growth system. Chem. Eng. J. Submitted.

Di Trapani, D., Mannina, G., Torregrossa, M., Viviani, G., 2008. Hybrid moving bed biofilm reactors: A pilot plant experiment. Water Sci. Technol. 57, 1539–1545.

Dong, Y., Fan, S.-Q., Shen, Y., Yang, J.-X., Yan, P., Chen, Y.-P., Li, J., Guo, J.-S., Duan, X.-M., Fang, F., Liu, S.-Y., 2015. A Novel Bio-carrier fabricated using 3D printing technique for wastewater treatment. Sci. Rep. 5, 1–10.

Dubois, M., Gilles, K.A., Hamilton, J.K., Rebers, P.A., Smith, F., 1956. Colorimetric method for determination of sugars and related substances. Anal Chem 28, 350–356.

Eldyasti, A., Nakhla, G., Zhu, J., 2012. Influence of particles properties on biofilm structure and energy consumption in denitrifying fluidized bed bioreactors (DFBBRs). Bioresour. Technol. 126, 162–171.

Falletti, L., Conte, L., Maestri, A., 2014. Upgrading of a wastewater treatment plant with a hybrid moving bed biofilm reactor (MBBR). AIMS Environ. Sci. 1, 45–52.

Goel, R., Kaldate, A., Murthy, S., Schraa, O., Stinson, B., 2011. Examining the phenomenon of self regulation of biofilm density under dynamic conditions using a biofilm model, in: WEFTEC 2011. Water Environment Federation, Los Angeles, pp. 5160–5177.

Habouzit, F., Hamelin, J., Santa-Catalina, G., Steyer, J.P., Bernet, N., 2014. Biofilm development during the start-up period of anaerobic biofilm reactors: The biofilm Archaea community is highly dependent on the support material. Microb. Biotechnol. 7, 257–264.

Hem, L.J., Rusten, B., Odegaard, H., 1994. Nitrification in a moving bed biofilm reactor. Water Res. 28, 1425–1433.

Holloway, T.G., Soares, A., 2018. Influence of internal fluid velocities and media fill ratio on submerged aerated filter hydrodynamics and process performance for municipal wastewater treatment. Process Saf. Environ. Prot. 114, 179–191.

Lackner, S., Holmberg, M., Terada, A., Kingshott, P., Smets, B.F., 2009. Enhancing the formation and shear resistance of nitrifying biofilms on membranes by surface modification. Water Res. 43, 3469–3478.

Le-Clech, P., Chen, V., Fane, T.A.G., 2006. Fouling in membrane bioreactors used in wastewater treatment. J. Memb. Sci. 284, 17–53.

Leyva-Díaz, J.C., Calderón, K., Rodríguez, F.A., González-López, J., Hontoria, E., Poyatos, J.M., 2013. Comparative kinetic study between moving bed biofilm reactor-membrane bioreactor and membrane bioreactor systems and their influence on organic matter and nutrients removal. Biochem. Eng. J. 77, 28–40.

Liu, Y., Tay, J.H., 2002. The essential role of hydrodynamic shear force in the formation of biofilm and granular sludge. Water Res. 36, 1653–1665.

Lowery, O.H., Rosebrough, N.J., Farr, A.L., Randall, R.J., 1951. Protein measurement with the folin phenol reagent. J. Biol. Chem. 193, 265–275.

Mahendran, B., Lishman, L., Liss, S.N., 2012. Structural, physicochemical and microbial properties of flocs and biofilms in integrated fixed-film activated sludge (IFFAS) systems. Water Res. 46, 5085–5101.

Mao, Y., Quan, X., Zhao, H., Zhang, Y., Chen, S., Liu, T., Quan, W., 2017. Accelerated startup of moving bed biofilm process with novel electrophilic suspended biofilm carriers. Chem. Eng. J. 315, 364–372.

Oberoi, A.S., Philip, L., 2017. Performance evaluation of attached biofilm reactors for the treatment of wastewater contaminated with aromatic hydrocarbons and phenolic

compounds. J. Environ. Chem. Eng. 5, 3852–3864.

Ødegaard, H., 2016. A road-map for energy-neutral wastewater treatment plants of the future based on compact technologies (including MBBR). Front. Environ. Sci. Eng. 10, 1–17.

Ødegaard, H., 2006. Innovations in wastewater treatment: The moving bed biofilm process. Water Sci. Technol. 53, 17–33.

Ødegaard, H., Gisvold, B., Strickland, J., 2000. The influence of carrier size and shape in the moving bed biofilm process. Water Sci. Technol. 41, 383–391.

Patel, A., Nakhla, G., Zhu, J., 2005. Detachment of multi species biofilm in circulating fluidized bed bioreactor. Biotechnol. Bioeng. 92, 427–437.

Pellicer-Nàcher, C., Smets, B.F., 2014. Structure, composition, and strength of nitrifying membrane-aerated biofilms. Water Res. 57, 151–161.

Regmi, P., Thomas, W., Schafran, G., Bott, C., Rutherford, B., Waltrip, D., 2011. Nitrogen removal assessment through nitrification rates and media biofilm accumulation in an IFAS process demonstration study. Water Res. 45, 6699–6708.

Rikmann, E., Zekker, I., Tenno, T., Saluste, A., Tenno, T., 2018. Inoculum-free start-up of biofilm- and sludge-based deammonification systems in pilot scale. Int. J. Environ. Sci. Technol. 15, 133–148.

Rikmann, E., Zekker, I., Tomingas, M., Tenno, T., Loorits, L., Vabamäe, P., Mandel, A., Raudkivi, M., Daija, L., Kroon, K., Tenno, T., 2014. Sulfate-reducing anammox for sulfate and nitrogen containing wastewaters. Desalin. Water Treat. 57, 3132–3141.

Rikmann, E., Zekker, I., Tomingas, M., Vabamäe, P., Kroon, K., Saluste, A., Tenno, T., Menert, A., Loorits, L., Rubin, S.S., Tenno, T., 2015. Comparison of sulfate-reducing and conventional Anammox upflow anaerobic sludge blanket reactors. J Biosci and Bioeng 118 (4), 426-433.

Salvetti, R., Azzellino, A., Canziani, R., Bonomo, L., 2006. Effects of temperature on tertiary

nitrification in moving-bed biofilm reactors. Water Res. 40, 2981–2993.

Siciliano, A., De Rosa, S., 2016. An experimental model of COD abatement in MBBR based on biofilm growth dynamic and on substrates' removal kinetics. Environ. Technol. (United Kingdom) 37, 2058–2071.

Syron, E., Casey, E., 2008. Membrane-aerated biofilms for high rate biotreatment: Performance appraisal, engineering principles, scale-up, and development requirements. Environ. Sci. Technol. 42, 1833–1844.

Szilágyi, N., Kovács, R., Kenyeres, I., Csikor, Z., 2013. Biofilm development in fixed bed biofilm reactors: experiments and simple models for engineering design purposes. Water Sci. Technol. 68, 1391–1399.

Tang, B., Yu, C., Bin, L., Zhao, Y., Feng, X., Huang, S., Fu, F., Ding, J., Chen, C., Li, P., Chen, Q., 2016. Essential factors of an integrated moving bed biofilm reactor-membrane bioreactor: Adhesion characteristics and microbial community of the biofilm. Bioresour. Technol. 211, 574–583.

Tang, B., Zhao, Y., Bin, L., Huang, S., Fu, F., 2017. Variation of the characteristics of biofilm on the semi-suspended bio-carrier produced by a 3D printing technique : Investigation of a whole growing cycle. Bioresour. Technol. 244, 40–47.

Tenno, T., Rikmann, E., Zekker, I., Tenno, T., L., Mashirin, A., 2016. Modelling equilibrium distribution of carbonaceous ions and molecules in a heterogeneous system of CaCO 3 – water–gas., in: Proceedings of the Estonian Academy of Sciences. p. 68.

Wiesmann, U., 1994. Biological nitrogen removal from wastewater. Adv. Biochem. Eng. Biotechnol. 51, 114–153.

Zekker, I., Rikmann, E., Kroon, K., Mandel, A., Mihkelson, J., Tenno, T., Tenno, T., 2017. Ameliorating nitrite inhibition in a low-temperature nitritation–anammox MBBR using bacterial intermediate nitric oxide. Int. J. Environ. Sci. Technol. 14, 2343–2356.

Zekker, I., Rikmann, E., Mandel, A., Kroon, K., Seiman, A., Mihkelson, J., Tenno, T.,

1 Toomas, T., 2016. Step-wise temperature decreasing cultivates a biofilm with high
2 nitrogen removal rates at 9°C in short-term anammox biofilm tests. Environ. Technol.
3 37, 1933–1946.

4 Zekker, I., Rikmann, E., Tenno, T., Vabamäe, P., Tomingas, M., Menert, A., Loorits, L.,
5 Tenno, T., 2012. Anammox Bacteria Enrichment and Phylogenic Analysis in Moving
6 Bed Biofilm Reactors. Environ. Eng. Sci. 29, 946–950.

7 Zhu, S., Chen, S., 2002. The impact of temperature on nitrification rate in fixed biofilters.
8 Aquac. Eng. 26, 221–237.

9 Zhu, Y., Zhang, Y., Ren, H. qiang, Geng, J. ju, Xu, K., Huang, H., Ding, L. li, 2015.
10 Physicochemical characteristics and microbial community evolution of biofilms during
11 the start-up period in a moving bed biofilm reactor. Bioresour. Technol. 180, 345–351.

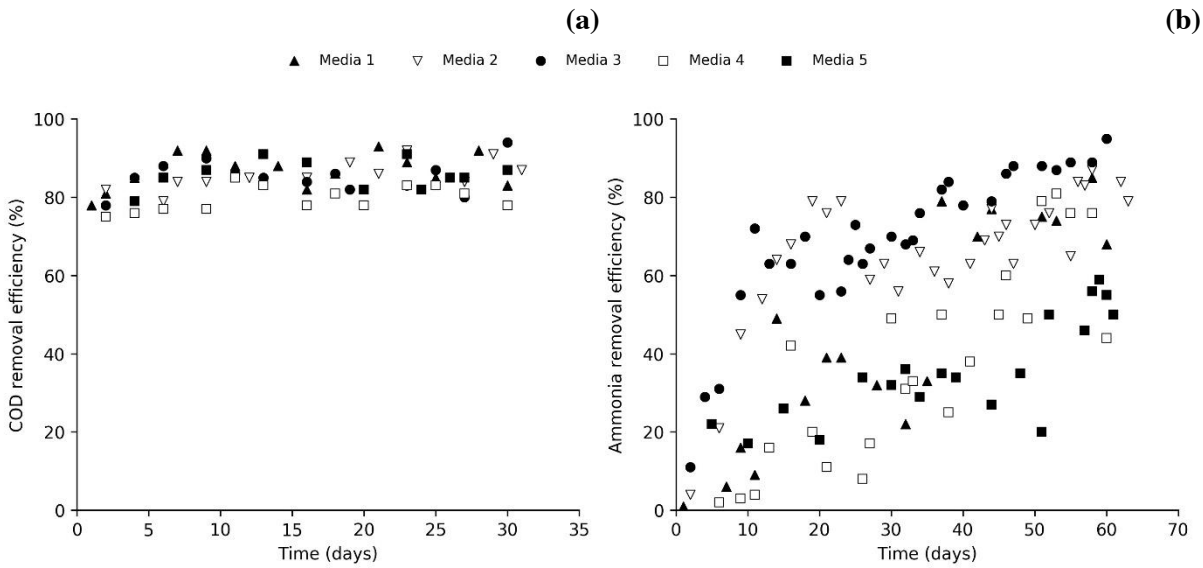

Figure 1 Removal efficiencies for obtainable COD (a) and ammonia (b) during start-up during operation with Media 1, 2, 3, 4 and 5, respectively.

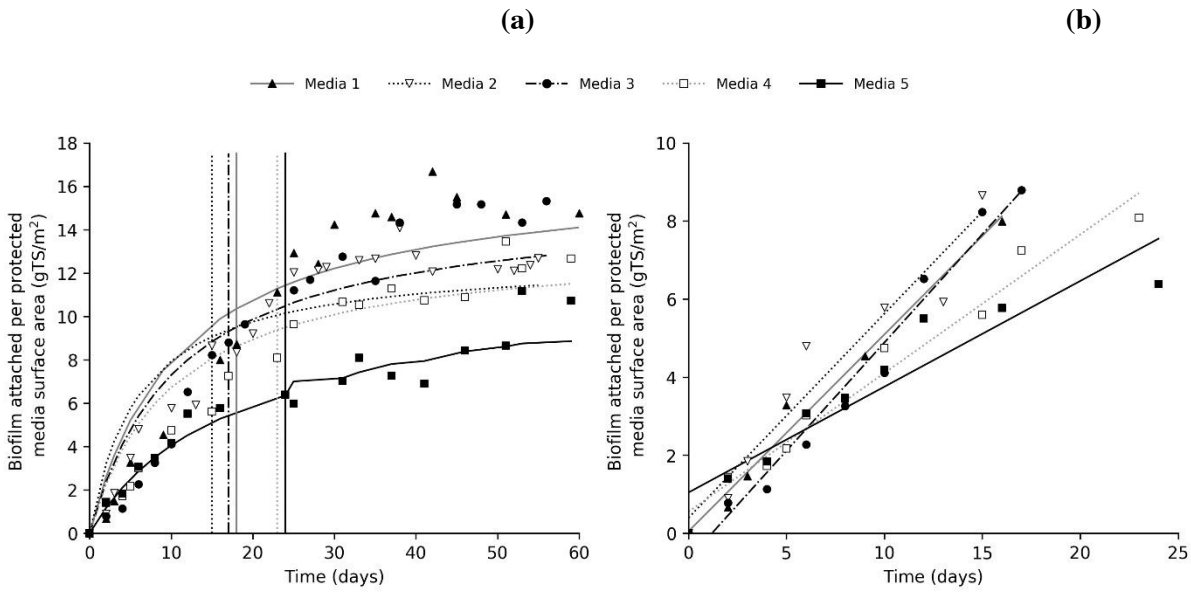

Figure 2 Biofilm attachment during 60 days of operation in cell 1 (COD removal) (a) and fitting of trend-line to calculate slope corresponding biofilm formation rate (b) during start-up.

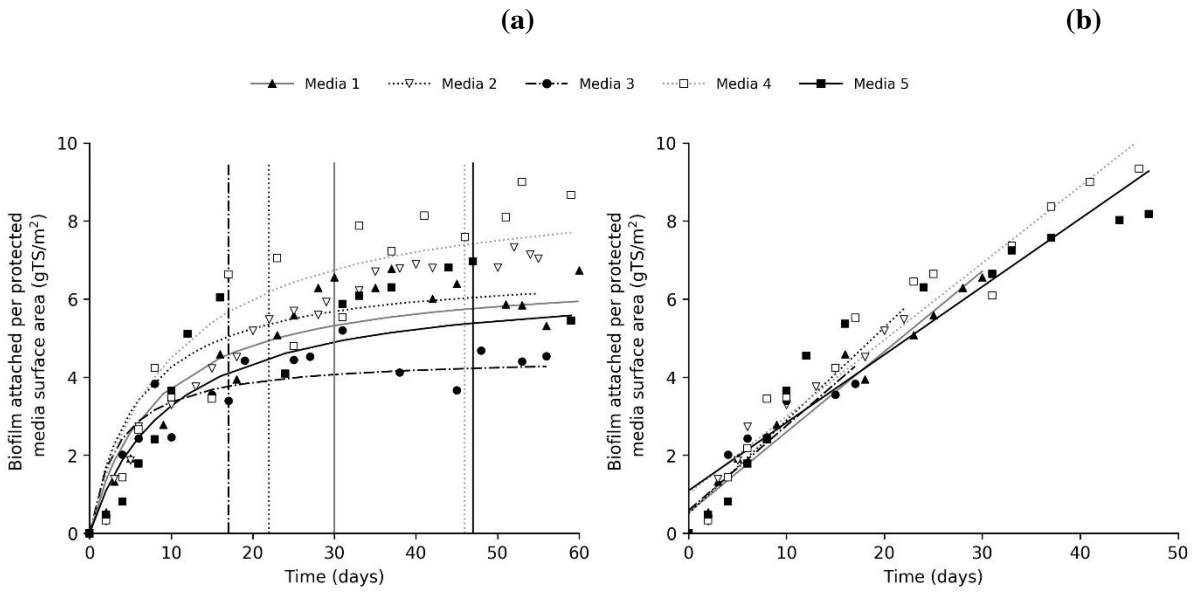

Figure 3 Biofilm attached during the 60 days of operation in Cell 3 (ammonia removal) (a) and fitting of trendline to calculate slope corresponding biofilm formation rate (b) during start-up.

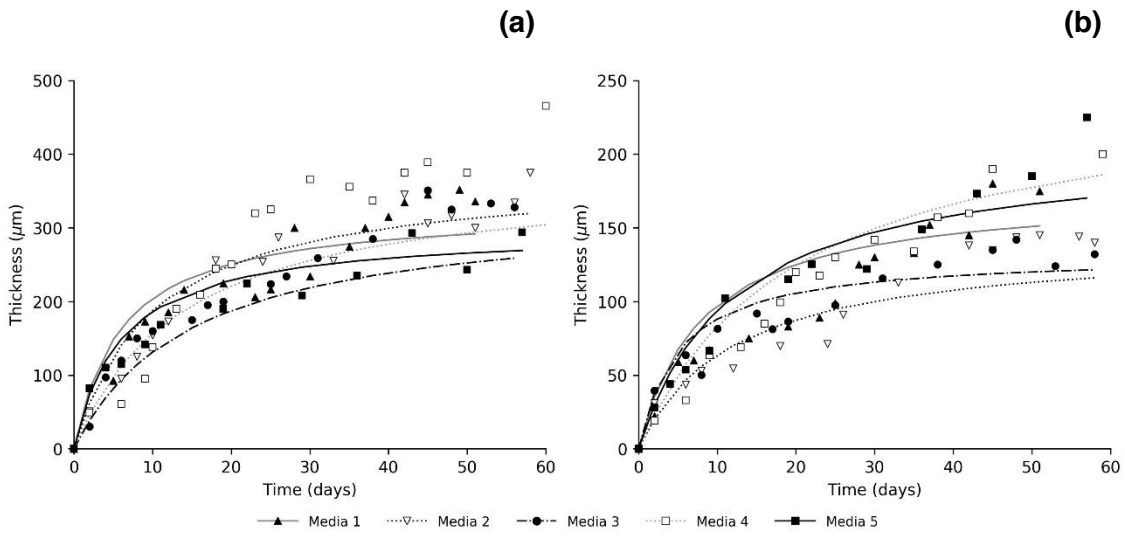

Figure 4 Biofilm thickness during 60 days of operation Cell 1(a) and Cell 3 (b).

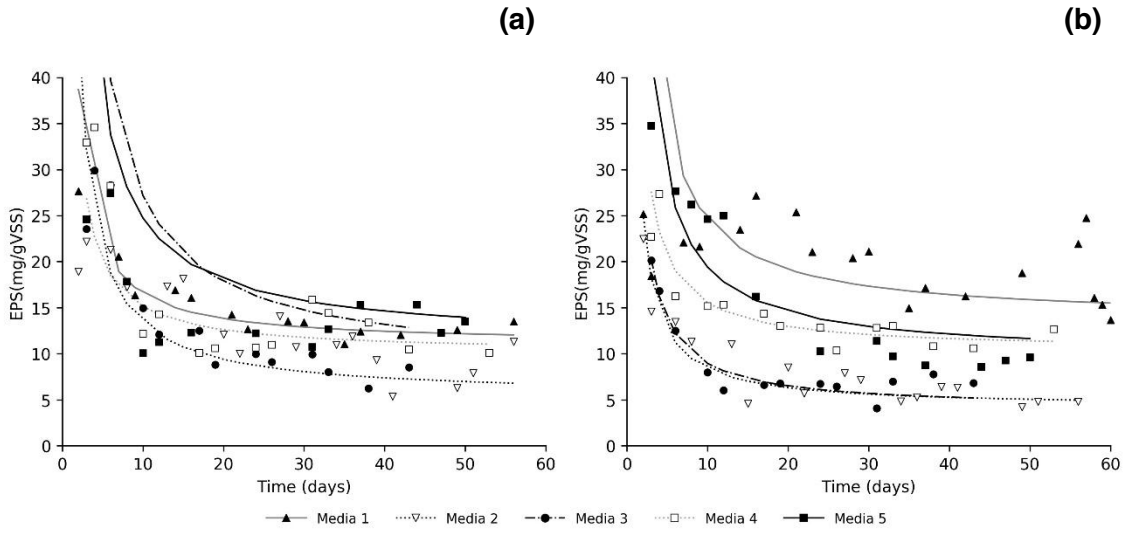

Figure 5 Total EPS values registered in Cell 1 (a) and Cell 3 (b) during 60 days of operation.

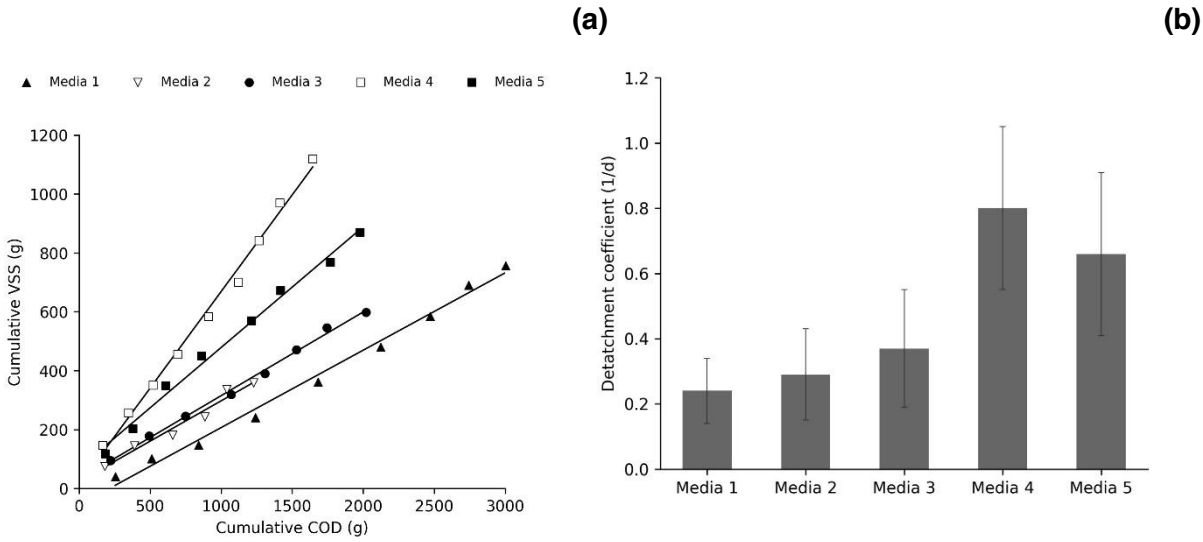

Figure 6 Biofilm yield (a) and biofilm detachment rate (b) calculated for the five media during COD start-up.

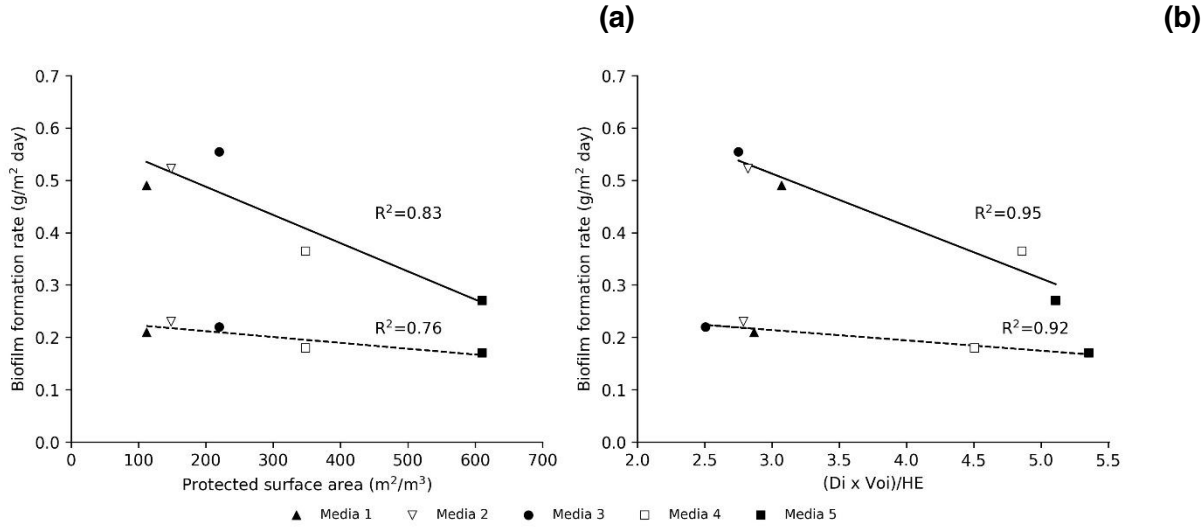

Figure *7* Correlation between biofilm formation rate and protected surface area (a) and combination of parameters (Di x Voi)/HE (b) during COD (-) and ammonia removal start-up (--).

Table 1

Media characteristics used in this study. Media 1 (Biofil), Media 2 (Bioball), Media 3 (Biomarble), Media 4 (Biopipe) and Media 5 (Biotube). Media was supplied by Warden Biomedia (http://www.wardenbiomedia.com).

Media	Total surface (m^2/m^3)	Protected surface area (m^2/m^3)	Shape	Dimensions		Voidage (%)	Material	Density (g/cm^3)
				Length (mm)	Diameter (mm)			
1	135	112	Spherical	65	95	95	Recycled polypropylene (PP)	0.97
2	220	148	Spherical	53	65	92		
3	310	220	Spherical	36	46	90		
4	600	348	Cylindrical	13	21.5	82.5		
5	1000	610	Cylindrical	8	12	80		

Table 2

Characterisation of the wastewater fed to the pilot plant operated with different media during start up.

Parameter	Unit	Media 1	Media 2	Media 3	Media 4	Media 5
Temperature	°C	15.1 ± 2.2	19.2 ± 2.2	20.9 ± 1.7*	13.8 ± 2.3*	13.1 ± 1.8
pH		7.6 ± 0.1	8.0± 0.2	7.7 ± 0.2	7.7 ± 0.3	8.1 ± 0.2
Total COD (tCOD)	mg/L	389 ± 71	257 ± 44	305 ± 32	236 ± 15	251 ± 24
Particulate COD (pCOD)	mg/L	317 ± 77	189 ± 41	234 ± 30	147 ± 20	187 ± 25
Soluble COD (sCOD)	mg/L	72 ± 7	68 ± 12	71 ± 5	89 ± 11	63 ± 8
BOD_5	mg/L	143 ± 47	81 ± 28	125 ± 27	158 ± 39	148 ± 38
Soluble BOD_5 ($sBOD_5$)	mg/L	11 ± 6	18 ± 2	22 ± 4	37 ± 8	32 ± 9
TSS	mg/L	225 ± 54	154 ± 88	205 ± 45	162 ± 33	202 ± 78
Ammonia (NH_4^+-N)	mg/L	35 ± 5	34 ± 11	36 ± 3	38 ± 6	31 ± 5

*Due to temperature variability, temperature for Media 4 and 5 were statistically different from Media 1, 2 and 3 ($p \leq 0.05$